

PAPER • OPEN ACCESS

A novel method for 3D reconstruction of blood vessels

To cite this article: Shengyu Lu 2021 *J. Phys.: Conf. Ser.* **1732** 012110

View the [article online](#) for updates and enhancements.

You may also like

- [Biomaterials for revascularization and immunomodulation after spinal cord injury](#)
Agnes E Haggerty, Inés Maldonado-Lasunción and Martin Oudega
- [Bioprinting small diameter blood vessel constructs with an endothelial and smooth muscle cell bilayer in a single step](#)
Lei Xu, Mathew Varkey, Adam Jorgensen et al.
- [Development of a technique to measure local scattering in turbid media using backscattered light at the surface for noninvasive turbidity evaluation of blood in subcutaneous blood vessels](#)
Shiyang Liang and Koichi Shimizu



DISCOVER
how sustainability
intersects with
electrochemistry & solid
state science research

A novel method for 3D reconstruction of blood vessels

Shengyu Lu*

Software School, Xiamen University, Xiamen, China

*Corresponding author e-mail: lu.s.y@foxmail.com

Abstract. With the development of computer technology, computer-aided diagnosis has been greatly improved. Computer-aided diagnosis can help doctors diagnose with medical imaging and other technique. Cardiovascular disease(CVD) lead to death with high probability. The computer-aided toward blood vessel is necessary. In this paper, we propose a novel method for 3D reconstructing of blood vessels. We calculate the volume data of blood vessels using an implicit modeling method based on the scanned blood vessel images, and establish a 3D model for blood vessels. Compared with existing methods, our method can obtain the surface and internal information of blood vessels accurately based on the implicit function method. The experimental results reflect that our method can implement 3D reconstruction of blood vessels with high accuracy and smoothness.

1. Introduction

Computer-aided diagnosis includes multiple technologies such as medical imaging, computer graphics, virtual reality and clinical medicine[1]. It can help doctors effectively in disease diagnosis[2], surgical planning, virtual surgical simulation, and reduce the risk of surgery. It can also improve the accuracy and effectiveness of disease diagnosis and treatment[3], and reduce the patient's pain and recovery cycle[4]. Currently, the main medical imaging technology includes Computed Tomography (CT), B-ultrasound scanning images, digital X-ray images, Magnetic Resonance Imaging (MRI)[5] and so on[6]. However, due to the limitations of display devices of medical imaging devices and several conditions, human eyes cannot make judgments accurately on some regions of medical images[7]. Image processing technology can diagnose medical images by improving the sharpness of the original image and highlighting the important regions. Therefore, image processing technology has been widely used in medical imaging research.

Image processing techniques include image restoration, segmentation, reconstruction, and enhancement[8]. Among them, image segmentation technology is the key technology in medical imaging and analysis. Medical image segmentation aims to separate the organ tissue of interest from the medical image, and analyze the physiological, pathological, physical and anatomical information by extracting the features of some interested regions.

Vascular diseases have a high incidence with the improvement of people's quality of life, and have big threat to human health. Segmentation of blood vessels from medical images has great significance for the diagnosis of vascular diseases. Besides, due to the variety of vascular variability, it is easy to cause major bleeding in the surgery if the shape and structure of vascular variability cannot be mastered before surgery. In order to judge the structure and function of the cardiovascular system, doctors often used clinically to obtain the shape and location of blood vessels with angiography. However, this technique provides a 2D image of blood vessels. In order to observe the blood vessels in



omnidirectional and accurate, assist in clinical diagnosis and surgical treatment, the 3D visualization of blood vessels has been applied since the 1990s[9], and it is first applying in thoracic surgery. Segmentation and 3D visual reconstruction of blood vessels from medical images can help doctors master the structure and function of blood vessels and play an important role in treatment planning.

Recently 3D printing technology has developed rapidly, and it can make any shape of entities to reduce its structural complexity. 3D printing has been used in many fields of medicine, including vascular surgery, which can help doctors master the structure of patients' blood vessels and conduct simulation experiments. Especially for rare patients, simulated surgery through vascular model from 3D printing can improve the successful rate and reduce the risk of surgery. Our method implements 3D reconstruction of blood vessels towards 3D printing.

2. Background and related work

3D reconstruction of blood vessels uses the computer technology to represent the geometric information of blood vessels. It segments the vascular images, extracts features, and digitally represents the geometric information of the blood vessels through points, lines, planes. By reconstructing the geometry of the blood vessels, it is possible to locate the lesion more accurately and perform quantitative analysis. 3D visualization of vascular disease often plays an important role in the diagnosis and treatment of vascular disease in minimally invasive treatment. Besides, visualization of different situations of the vascular model may be applicable to different cases. The vascular system is a complex network of blood vessels, so 3D visualization of vascular models has a big challenge. Traditional medical volume data visualization techniques such as isosurface rendering, direct volume rendering, or maximum intensity projection (MIP) can not meet the requirements of medicine due to image noise and the limited resolution of Computed Tomography (CT) or Magnetic Resonance (MR)[10]. MIP can not reflect depth relationships correctly, while small blood vessels disappear completely. Reconstruct the vascular structure, according to the geometric properties of the blood vessels such as the midline, diameter, and curvature. Reconstructed the geometry of blood vessels can help greatly reduce aliasing and discontinuities caused by derives and achieve high visual quality of vascular structures[11]. The primary part of 3D reconstruction of vascular images is to segment the blood vessels[12].

In recent years, medical image segmentation technology has developed rapidly. It is represented by the active contour model and the level set method[13]. The level set method was proposed by Osher and Sethina[14]. They defined the level set function of the curve, which used the zero level set of high one-dimensional function to describe the dynamically changing of the curve. Then the level set function used the display function to evolve the curve and describe the dynamic process.

We use the hybrid level set method to represent the geometry of blood vessels. We adopt the implicit contour method to describe the contour curve of objects without using the display method. We represent the blood vessels by the zero-level set of high-dimensional level set functions. It is that our evolution curve is implicitly represented on a surface. The curves and surfaces can be numerically calculated on the fixed Cartesian network and need not to represent these objects with parameters. Therefore, the hybrid level set method can handle the topology changes well during the evolution process.

3. Method

We use the implicit model to reconstruct the 3D model of blood vessels. We first fit the key points of blood vessel section, then combine the section contours into blood vessel branches, and merge these blood vessel branches into a complete 3D model of the blood vessel. In addition, in order to ensure the integrity of the blood vessels, we extend the outlet and entrance of the blood vessels.

3.1. Implicit surface description

We use the implicit function to represent the blood vessels as a set of blobs. Each element can be represented by point energy. Therefore, the blood vessel can be regarded as an influence field, and the energy decreases as the distance increases. The influence domain function $\phi(r)$ can be defined as:

$$\varphi(r) = e^{-ar^2} \quad (1)$$

Where, r represents the distance between the point and energy source and a is a parameter of $\varphi(r)$.

We can describe the implicit surface as a weighted set. We let $\{P_i\}_{i=1}^n$ represent the center of it, and the set can be represented as $\sum_{i=1}^n \rho_i \varphi_i(r)$. The implicit surface defines as:

$$F(P) = \sum_{i=1}^n \rho_i \varphi_i(\|P - P_i\|) + \omega(P) \quad (2)$$

Where, ρ_i is the parameter of $F(P)$ function and n represents the number of energy points. We let $p(x, y, z)$ represent a point in 3D space and P_i represent the i th energy point. $\omega(P)$ represents a polynomial.

3.2. Key points of the blood vessels section

We use the local Frenet function to fit the key points of each cross section during the blood vessels segmentation process. We need to calculate the Frenet based on the axis data of blood vessels. The Frenet frame is a field built on the curve. We use the unit vector of the curve to build a unit of orthogonal frame field. We let $S(s)$ represent the curve and $S(s_i)$ represents the i th point on the curve, as shown in Figure 1.

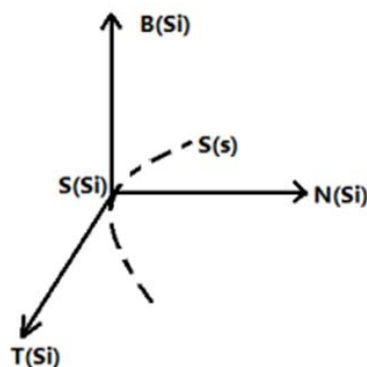


Figure 1. The framework of Frenet.

The Frenet defines as:

$$Frenet = \begin{cases} T(s_i) = \frac{S'_{(s_i)}}{\|S'_{(s_i)}\|} \\ N(s_i) = \frac{S''_{(s_i)}}{\|S''_{(s_i)}\|} \\ B(s_i) = T(s_i) * N(s_i) \end{cases} \quad (3)$$

Where, $T(s_i)$ 、 $N(s_i)$ 、 $B(s_i)$ represent the unit vectors in three orthogonal directions respectively. $S'_{(s_i)}$ represents the first derivative of the tangent vector of the curve on the point $S(s_i)$. $\|S'_{(s_i)}\|$ represents its modulus length. Likely, $S''_{(s_i)}$ represents the second derivative of the tangent vector and $\|S''_{(s_i)}\|$ is its modulus length.

The points whose value more than 0 can be identified. Therefore, The points with value more than 0 in the cross section are regarded as the key points of the blood vessels. We let $\{P_i^+\}(B, n)$ denote a set of contour points of the coordinate plane B_n extracted from the blood vessel section. The implicit curve can be represented as:

$$C(P^+) = \sum_{i=1}^n \rho_i \varphi_i(\|P^+ - P_i^+\|) + \omega(P^+) = 0 \quad (4)$$

3.3. Blood vessel branches

We map the distance along the central axis of the blood vessel, and mixed all the cross-sectional profiles with implicit markers using the local conformal spline method to build the blood vessel

branches. A 2D cross section is extruded along the central axis by distance and maps to form a 3D implicit surface. The cross section is formed in the Frenet. We conduct the distance mapping first and calculate the central axis point $S(s_0)$ which is closest to point P.

$$\|P - S(s_0)\| = \min(\|P - S(s)\|) \quad (5)$$

Then we convert the point P in 3D space into the point $P^+(b, n, t)$ in the tangent space of Frenet. It defines as following:

$$\begin{cases} b = \overrightarrow{p - S(s_0)} * B(s_0) \\ n = \overrightarrow{p - S(s_0)} * N(s_0) \\ t = s_0 \end{cases} \quad (6)$$

The cross-sectional profiles in Frenet are represented by the distance map as follows:

$$\begin{cases} b = X(x, y, z) \\ n = Y(x, y, z) \\ t = Z(x, y, z) \end{cases} \quad (7)$$

There, the extruded implicit surface of can define as:

$$F(x, y, z) = C(P^+(X, Y, Z)) = 0 \quad (8)$$

We define an implicit surface model ,which is the weighted sum of the sequence of cross-sectional profiles along the central axis of the blood vessel. So it is corresponding to the Frenet space and defines as:

$$f(b, n, t) = \sum_{j=1}^L C(P^+(b, n, t)) B_j(t - s_j) \quad (9)$$

Where, $C(P^+(b, n, t))$ represents the implicit section based on the j th center point and $B_j(t - s_j)$ represents the conformal implicit spline function based on the j th center point. L is the number of cross sections and s_j is the list of nodes of the parameter position on the central axis $S(s)$.

Then we convert the result into representation in European space. For the central axis S , using the distance mapping, the implicit surface model in the Frenet space can be converted to a 3D space representation by following:

$$F(x, y, z) = f(b, n, t) == f(X(x, y, z), Y(x, y, z), Z(x, y, z))=0 \quad (10)$$

3.4. Combine blood vessel branches

We use the extended smoothing maximum function to mix different vessel branches to construct the complete blood vessels. The extended smoothing maximum function defines as:

$$\max_{n,\sigma}(x, y) = \frac{1}{2}(x + y + |x - y|_{n,\sigma}) \quad (11)$$

Where, σ represents the parameter of the extended smoothing maximum function and n is the number of functions.

We let F_1 and F_2 represent the branches of blood vessels implicitly constructed by the axes of different blood vessels. Then we combine the two implicit shapes smoothly as follows:

$$F_{blend} = \max_{n,\sigma}(F_1, F_2) = \frac{1}{2}(F_1 + F_2 + |F_1 - F_2|_{n,\sigma}) \quad (12)$$

3.5. Extend the entrance and exit

When take the cross-section at the entrance and exit of the blood vessel, we extend the entrance and exit of the blood vessel to preserve the structure of original blood vessel as much as possible. We extend the straight line of the blood vessel to make the subsequent operations more convenient. We first extend the central axis of the blood vessel, then find the last two points $M(x_1, y_1, z_1)$ and $N(x_2, y_2, z_2)$ of each central axis branch, and connect them into a straight line. The equation defines as[17]:

$$\frac{x-x_2}{x_2-x_1} = \frac{y-y_2}{y_2-y_1} = \frac{z-z_2}{z_2-z_1} \quad (13)$$

We extract some points on the line according to center line on the extension direction of the blood vessel, and add it to the end of the central axis. We use the spline function to spline the central axis, and then use the extension method of blood vessels introduced in implicit modeling. We extend the end of each branch along the end of the central axis.

4. Experiment

We performed experiments in the windows system and used Matlab to reconstruct the 3D model of blood vessels. We first processed the vascular image data and obtain the vascular data file in .mat format.

Then we imported the central axis data of blood vessels and used the spline interpolation function to draw the central axis and represent the blood vessel data, as shown figure 2:

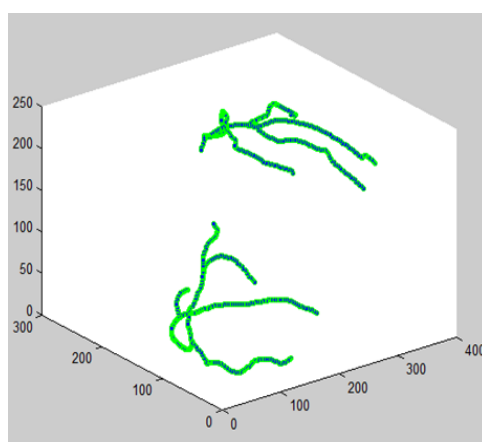


Figure 2. The central axis of blood vessels.

We extended the exit and entrance of the blood vessel using a straight line, as shown in the Figure 2 above, which is the central axis of the original blood vessel. The Figure 3 is the image of the extended entrance to the blood vessel and Figure 4 is the image of the extended exit and entrance of the blood vessel.

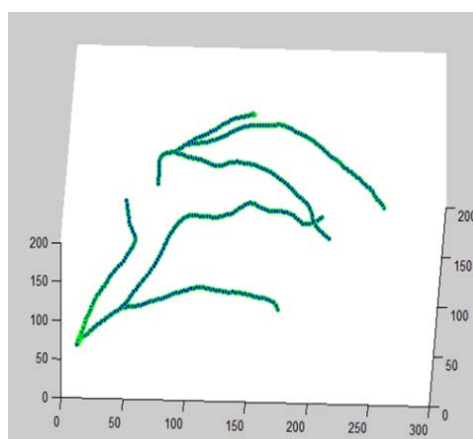


Figure 3. The extended entrance to the blood vessel.

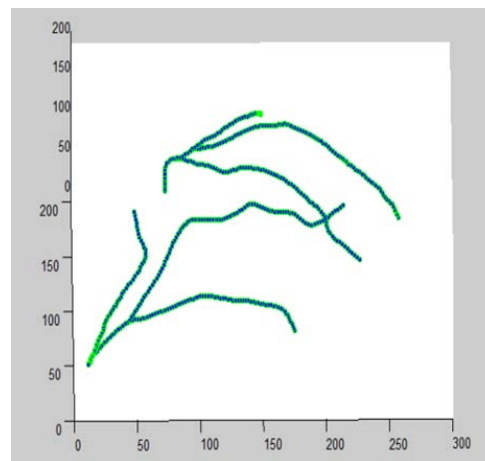


Figure 4. The extended exit and entrance to the blood vessel.

We extended the exit and entrance of the blood vessel, and reconstructed the blood vessel and extracted the blood vessel isosurface with a value of 0.5. We can see a new blood vessel segment at the entrance and exit of the blood vessel in Figure 4.

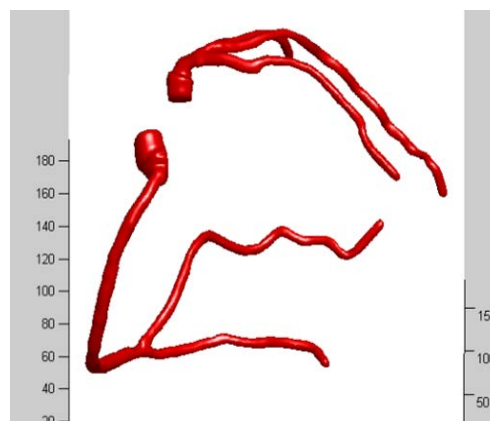


Figure 5. The extended result.

5. Conclusion

In this paper, we propose a novel method to reconstruct a 3D model of for blood vessels. We use an implicit method that uses a mixed level set method and combines the surface and internal information of the blood vessels. We extract the key points of the blood vessel section, then combine the section contours into vessel branches, and merge these blood vessel branches into the complete 3D model for the blood vessels. In addition, we extend the exit and entrance of blood vessels to ensure the integrity of the vascular structure. Our method can accomplish 3D reconstruction of blood vessel images and implement accurate and smooth 3D models, which is meaningful for the computer-aided diagnosis.

References

- [1] O. F. Ahmad et al., "Artificial intelligence and computer-aided diagnosis in colonoscopy: current evidence and future directions," *The Lancet Gastroenterology & Hepatology*, vol. 4, no. 1, pp. 71–80, Jan. 2019.
- [2] O. Faust et al., "Computer aided diagnosis of Coronary Artery Disease, Myocardial Infarction and carotid atherosclerosis using ultrasound images: A review," *Physica Medica*, vol. 33, pp. 1–15, Jan. 2017.
- [3] Y. Hagiwara et al., "Computer-aided diagnosis of glaucoma using fundus images: A review," *Computer Methods and Programs in Biomedicine*, vol. 165, pp. 1–12, Oct. 2018.

- [4] D. E. Diamantis, D. K. Iakovidis, and A. Koulaouzidis, "Look-behind fully convolutional neural network for computer-aided endoscopy," *Biomedical Signal Processing and Control*, vol. 49, pp. 192–201, Mar. 2019.
- [5] G. Lemaître, R. Martí, J. Freixenet, J. C. Vilanova, P. M. Walker, and F. Meriaudeau, "Computer-Aided Detection and diagnosis for prostate cancer based on mono and multi-parametric MRI: A review," *Computers in Biology and Medicine*, vol. 60, pp. 8–31, May 2015.
- [6] S. Lu, "An Image Retrieval Learning Platform with Authentication System," in *2018 13th International Conference on Computer Science & Education (ICCSE)*, Colombo, 2018, pp. 1–5.
- [7] E. Mabrouk, A. Ayman, Y. Raslan, and A.-R. Hedar, "Immune system programming for medical image segmentation," *Journal of Computational Science*, vol. 31, pp. 111–125, Feb. 2019.
- [8] B. B. Traore, B. Kamsu-Foguem, and F. Tangara, "Deep convolution neural network for image recognition," *Ecological Informatics*, vol. 48, pp. 257–268, Nov. 2018.
- [9] Y.-C. Lai, Y.-S. Huang, D.-W. Wang, C.-M. Tiu, Y.-H. Chou, and R.-F. Chang, "Computer-Aided Diagnosis for 3-D Power Doppler Breast Ultrasound," *Ultrasound in Medicine & Biology*, vol. 39, no. 4, pp. 555–567, Apr. 2013.
- [10] V. Gupta et al., "Cardiac MR perfusion image processing techniques: A survey," *Medical Image Analysis*, vol. 16, no. 4, pp. 767–785, May 2012.
- [11] L. D. J. Fiederer et al., "The role of blood vessels in high-resolution volume conductor head modeling of EEG," *NeuroImage*, vol. 128, pp. 193–208, Mar. 2016.
- [12] X. Wang, X. Jiang, and J. Ren, "Blood vessel segmentation from fundus image by a cascade classification framework," *Pattern Recognition*, vol. 88, pp. 331–341, Apr. 2019.
- [13] N. Shervani-Tabar and O. V. Vasilyev, "Stabilized conservative level set method," *Journal of Computational Physics*, vol. 375, pp. 1033–1044, Dec. 2018.
- [14] W. Han, Z. Jin, L. Wang, M. Hu, Z. Wang, and Q. Peng, "Molecular field feature extraction and analysis with level set method," *Computers & Graphics*, vol. 32, no. 6, pp. 632–638, Dec. 2008.
- [15] S. Lu, H. Chen, X. Zhou, B. Wang, H. Wang, and Q. Hong, "Graph-Based Collaborative Filtering with MLP," *Mathematical Problems in Engineering*, vol. 2018, pp. 1–10, Dec. 2018.
- [16] Y. Hang, C. Derong, and G. Jiulu, "Object tracking using both a kernel and a non-parametric active contour model," *Neurocomputing*, vol. 295, pp. 108–117, Jun. 2018.
- [17] S. Lu, B. Wang, H. Wang, and Q. Hong, "A Hybrid Collaborative Filtering Algorithm Based on KNN and Gradient Boosting," in *2018 13th International Conference on Computer Science & Education (ICCSE)*, Colombo, 2018, pp. 1–5.